Eur. Phys. J. D **45**, 171–177 (2007)
DOI: 10.1140/epjd/e2007-00143-4

THE EUROPEAN PHYSICAL JOURNAL D

QED corrections and chemical properties of Eka-Hg

I. Goidenko[1,a], I. Tupitsyn[1], and G. Plunien[2]

[1] St. Petersburg State University, 198504 Ulyanovskaya 1, Petrodvorets, St. Petersburg, Russia
[2] Institut für Theoretische Physik, Technische Universität Dresden, Mommsenstrasse 13, 01062 Dresden, Germany

Received 15 November 2006 / Received in final form 17 February 2007
Published online 6 April 2007 –

Abstract. The influence of quantum electrodynamic (QED) corrections on the valence electrons in superheavy atoms with nuclear charge $Z \approx 112$ is studied within the effective local-potential approximation and the self-consistent approach. The results are obtained from a relativistic coupled-cluster calculation without inclusion of QED effects. The difference between the effective-potential and the self-consistent approach for the leading QED correction to the energy of the valence-electron levels in any superheavy atoms defines an inaccuracy of about 0.1% of the first ionization potential.

PACS. 31.30.Jv Relativistic and quantum electrodynamic effects in atoms and molecules

1 Introduction

Recent experimental success in the synthesis of superheavy nuclei [1–5] has provided strong indications for the existence of the so-called "island of stability" for neutron-rich nuclei with nuclear charge numbers in the region $Z \sim 112$. According to theoretical predictions, the half-life time for nuclei with proton numbers $Z \sim 108$ and neutron number $N \sim 162$, as well as for isotopes with $Z \sim 114$ and $N \sim 184$ could be very long. These pairs of proton and neutron numbers were supposed to correspond to filled proton and neutron shells. Neighboring nuclei close to these "magic numbers" of Z and N should be rather long-living as well. Presented in a graph (Z, N) (Fig. 1) such nuclei are supposed to form the island of stability.

From the variety of experimental investigations on the synthesis of long-living superheavy nuclei, we mention here only the results reported in some recent papers. According to [2], for instance, the half-life time for the isotope Hs ($Z = 108$) is found to be of about several seconds. Similarly, for the two isotopes with nuclear charge numbers $Z = 111$ [3] and $Z = 114$ [4] the corresponding time periods of half-decay turned out to be of about one second, too.

A further breakthrough in the synthesis of long-living isotopes with proton number $Z = 112$ — so-called Eka-Hg (E112), which was supposed to belong to the group 12 in the Mendeleyev Periodic Table (MPT) — has been reported from the Flerov Laboratory of Nuclear Reactions (Dubna). The half-decay times of several identified isotopes of Eka-Hg up to about a few minutes [5] have been deduced, which appeared to be also in a beautiful agreement with present theoretical predictions (see, for instance, Tab. 2 in Ref. [6]). The successful formation of such superheavy nuclei and the preparation of neutral atoms allowed for investigation of their chemical characteristics as well. According to these findings the superheavy element with $Z = 112$ behaves more like a homologue of the noble gas radon (Rn) rather than mercury (Hg).

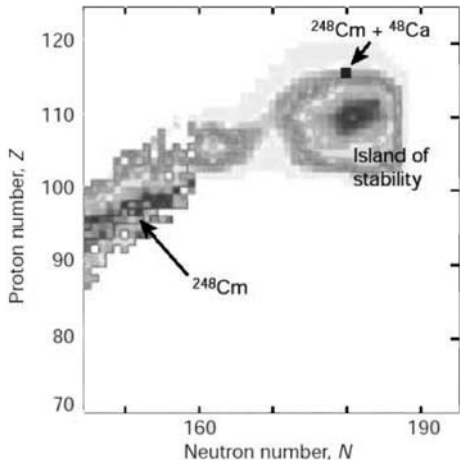

Fig. 1. The island of stability. Dark figures in the center indicate stable, long-living nuclei; the border of a big cloud represent nuclei, which decay shortly after their formation. The heaviest known element with $Z = 116$ (depicted as a dark square) is formed in reaction of ^{248}Sm and ^{48}Ca and which have the half-life time 50 ms.

The valence shell of the Eka-Hg atom contains only two electrons, which allows for considerable simplifications in corresponding atomic structure calculations. A pioneering paper about such atoms is reference [7], where electron binding energies and X-ray energies for the superheavy elements with $Z = 114, 126$ and $Z = 140$ have been calculated within a relativistic self-consistent

[a] e-mail: igor_g@landau.phys.spbu.ru

(Hartree-Fock-Slater) approach. As can be seen from Figure 1, the isotopes of the element E114 could be located on top of the island of stability.

Usually, most of the atomic structure calculations for superheavy elements do not account for QED effects. So far, only in a few more recent articles attempts were undertaken to study the influence of QED corrections on the binding energy of valence electrons in superheavy atoms [8,9] and to explore their impact on chemical properties of such elements.

Within this paper we are going to address related questions. We show that QED corrections should be taken into account in exact evaluations of the energy levels of valence electron in superheavy elements. Moreover, the magnitude of the difference between results obtained by incorporation of QED effects within the self-consistent and within local potential approaches, respectively, turns out to be of about the same order as the inaccuracy of relativistic calculations where QED corrections are neglected.

The paper is organized as follows: the most important one-loop QED contributions are considered in Section 2. Particular emphasize is lead on the description of the method employed for a systematic account of QED effects in the superheavy atoms (Sect. 3). Corresponding numerical results and the role of QED corrections for the level energy of outer-shell electrons is subsequently discussed. A simple approach for the construction of effective local potentials for valence electrons is explained in the Appendix.

Atomic units $e = m = \hbar = 1$, where $-e$ is the charge of the electron, m is its mass and $\hbar$ is the Planck's constant, are mainly used this paper.

2 Leading one-loop QED corrections

This section reviews the evaluation scheme for the dominant one-loop QED corrections (self energy and vacuum polarization) to the level energy as it will be applied below to outer-shell electrons in superheavy atoms. While the vacuum-polarization effect appears as modification of the external potential, which allows for immediate incorporation within relativistic many-body approaches, the self-energy effects — since they are inherently nonlocal — require more efforts. A recent attempt to account for QED corrections in many-electron systems [9] provides an estimate of self-energy effects within the framework of the GRASP code. However, the accuracy of such a treatment is very difficult to determine. Accordingly, we prefer a more transparent procedure by evaluating the one-electron self energy within a local potential approach. Questions about the accuracy will be addressed in Section 3.

2.1 Self-energy correction

For electron states in heavy atoms the parameter $Z\alpha$ cannot be considered as being small. Accordingly, accurate evaluations of QED self-energy corrections require all-order calculations with respect to $Z\alpha$. Moreover, in the case of heavy atoms one is faced with the situation that the effective potentials describing the electron interaction with the nucleus are rather short-range and the interaction occurs when the outer shell electrons penetrate deeply into the core.

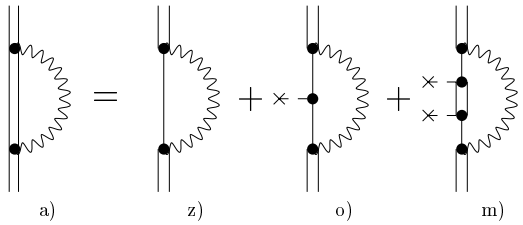

Fig. 2. The expansion of the electron SE graph in powers of the effective local potential V. The double solid line denotes an electron in the effective local potential V, the ordinary solid line denotes the free electron propagator and the wavy line denotes the photon propagator. The dashes line with the cross at the end denotes the interaction with the effective local potential V.

The method that enabled to overcome this difficulty has been first introduced in [10] and applied to the evaluation of the self energy (SE) for K-shell electrons in a mercury atom. The general idea of the method is based on the potential expansion. The Feynman graph representing the expansion of the SE of a bound electron in the state a is depicted in Figure 2. The divergencies involved appear in the first two terms, called "zero-potential" (z) and "one-potential" (o) terms, respectively. The third term, so-called "many-potential" (m) term, is finite but the most difficult one for numerical evaluations. The evaluation of this term together with renormalization may be achieved according to the scheme presented in [10] based on rearrangements of the three terms of the potential expansion: $\Delta E_a^{\rm SE} = \Delta E_a^{(\rm z)} + \Delta E_a^{(\rm o)} + \Delta E_a^{(\rm m)}$ The renormalized self-energy shift of a level a appears as

$$\Delta E_a^{\rm SE,ren} = \Delta E_{\rm a}^{\rm ren(z)} + \Delta E_{\rm a}^{\rm ren(o)} + \Delta E_{\rm a}^{\rm ren(m)}, \quad (1)$$

where the label a denotes the electron state in the atom. According to Figure 2 the renormalized expressions for $\Delta E_{\rm a}^{\rm ren(z)}$ (part (z) of Fig. 2) and $\Delta E_{\rm a}^{\rm ren(o)}$ (part (o) of Fig. 2) are obtained by means of the subtractions scheme [10]

$$\Delta E_a^{\rm ren(z)} = \Delta E_a^{(\rm z)} - \Delta E_a^{(\rm z1)} - \Delta E_a^{(\rm z2)}, \quad (2)$$

$$\Delta E_a^{\rm ren(o)} = \Delta E_a^{(\rm o)} - \Delta E_a^{(\rm o1)}, \quad (3)$$

where $\Delta E_a^{(zi)}$, $\Delta E_a^{(oi)}$ $(i = 1, 2, ...)$ denote the terms of the Taylor expansion of the lowest-order self-energy operator around the mass shell.

The Ward identity implies $\Delta E_a^{(\rm z2)} = -\Delta E_a^{(\rm o1)}$. Within the direct potential expansion approach the analytically known expressions for the renormalized contributions $\Delta E_a^{\rm ren(z)}$ and $\Delta E_a^{\rm ren(o)}$ are employed. They can be obtained from the corresponding S-matrix elements in the

well-known momentum-space representations. The renormalized expression for the zero-potential term reads

$$\Delta E_a^{\mathrm{ren(z)}} = \int \overline{\Psi}_a(\mathbf{p}) \Sigma^{\mathrm{ren}}(\mathbf{p}, E_a) \Psi_a(\mathbf{p})\, d^3p, \qquad (4)$$

where $\Sigma^{\mathrm{ren}}(\mathbf{p}, E_a)$ is the renormalized free electron self-energy insertion (see Ref. [12]), $\Psi_a(\mathbf{p})$ is the bound-electron wave function in the momentum space. The general gauge-dependent expression for $\Sigma^{\mathrm{ren}}(p)$ appears to be [11]

$$\Sigma^{\mathrm{ren}}(p) = \frac{\alpha}{4\pi}(\not{p} - m)\left\{\frac{m^2}{p^2}\ln\left|\frac{p^2-m^2}{m^2}\right|\left(d_0\frac{p^2}{m^2} - 3\right)\right.$$
$$- \frac{1}{2}\ln\frac{\lambda^2}{m^2}(6 - 2d_0) - d_0$$
$$\left. + \frac{\not{p}}{m}\left[\frac{m^2}{p^2}\ln\left|\frac{p^2-m^2}{m^2}\right|\left(d_0\frac{p^2}{m^2} - 3\right) + d_0\frac{m^2}{p^2}\right]\right\}, \qquad (5)$$

where m is the electron mass, $p \equiv (\mathbf{p}, p_0)$, $p_0 = E_a$, $\not{p} = p^\mu\gamma_\mu$ and γ_μ denotes the Dirac matrices.

The appearance of a photon mass λ in equation (5) implies the presence of an infrared divergency after renormalization, d_0 is the parameter defining the gauge. In the Feynman gauge $d_0 = 1$ and in the Fried-Yennie gauge $d_0 = 3$. One can see that in the Fried-Yennie gauge the infrared divergency is absent. However, calculations performed within this gauge become more complicated for the higher-order terms of the potential expansion. Therefore, the Feynman gauge will be employed.

The renormalized one-potential term is given by

$$\Delta E_a^{\mathrm{ren(o)}} = \int \overline{\Psi}_a(\mathbf{p}) \Lambda_0^{\mathrm{ren}}(\mathbf{p}E_a; \mathbf{q}E_a) eV(\mathbf{p} - \mathbf{q})$$
$$\times \Psi_a(\mathbf{q})\, d^3p d^3q. \qquad (6)$$

An expression for renormalized free vertex function $\Lambda_0^{\mathrm{ren}}(\mathbf{p}E_a; \mathbf{q}E_a)$, which is most convenient for numerical evaluations, is obtained within the Feynman gauge [12]

$$\Lambda_0^{\mathrm{ren}}(\mathbf{p}E_a; \mathbf{q}E_a) = \tilde{\Lambda}_0^{\mathrm{ren}}(\mathbf{p}E_a; \mathbf{q}E_a) + \ln\frac{\lambda^2}{m^2}, \qquad (7)$$

where the infrared-finite part reads

$$\tilde{\Lambda}_0^{\mathrm{ren}}(\mathbf{p}E_a; \mathbf{q}, E_a) = \gamma_0[4\tilde{C}_{24} - 2 + 2m_e^2 C_0 - 4pp'(C_0 + C_{11}$$
$$+ C_{12} + C_{23}) - 2p^2(C_{11} + C_{21}) - 2p'^2(C_{12} + C_{22})]$$
$$+ \not{p}p_0[4(C_{11} + C_{21})] + \not{p}p_0'[4(C_0 + C_{11} + C_{12} + C_{23})]$$
$$+ \not{p}'p_0[4(C_0 + C_{11} + C_{21} + C_{23})] + \not{p}'p_0'[4(C_{12} + C_{22})]$$
$$- \not{p}\gamma_0\ \not{p}'[2(C_0 + C_{11} + C_{12})]$$
$$- p_0[4m_e(C_0 + 2C_{11})] - p_0'[4m_e(C_0 + C_{12})]. \qquad (8)$$

Here C_0, C_{ij} denote the Feynman parameter integrals:

$$m^2 C_0 = \int_0^1 dy \frac{1}{a}\ln\left(\frac{a+b}{b}\right), \qquad (9)$$

$$m^2 C_{11} = -\int_0^1 dy \frac{y}{a}\left[1 - \frac{b}{a}\ln\left(\frac{a+b}{b}\right)\right], \qquad (10)$$

$$m^2 C_{12} = -\int_0^1 dy \frac{1-y}{a}\left[1 - \frac{b}{a}\ln\left(\frac{a+b}{b}\right)\right], \qquad (11)$$

$$m^2 C_{21} = \int_0^1 dy \frac{y^2}{a}\left[\frac{1}{2} - \frac{b}{a} + \left(\frac{b}{a}\right)^2\ln\left(\frac{a+b}{b}\right)\right], \qquad (12)$$

$$m^2 C_{22} = \int_0^1 dy \frac{(1-y)^2}{a}\left[\frac{1}{2} - \frac{b}{a} + \left(\frac{b}{a}\right)^2\ln\left(\frac{a+b}{b}\right)\right], \qquad (13)$$

$$m^2 C_{23} = \int_0^1 dy \frac{y(1-y)}{a}\left[\frac{1}{2} - \frac{b}{a} + \left(\frac{b}{a}\right)^2\ln\left(\frac{a+b}{b}\right)\right], \qquad (14)$$

$$C_{24} = \frac{1}{4}\left\{1 - \int_0^1 dy \frac{b}{a}\left[1 - \frac{b}{a}\ln\left(\frac{a+b}{b}\right)\right] - \int_0^1 \ln(a+b)\right\} \qquad (15)$$

with the abbreviations $b = y\rho - (1-y)\rho'$ and $a + b = 1 - y(1-y)k^2/m^2$, $k^2 = (\mathbf{p} - \mathbf{q})^2$, $\rho = (m^2 + p^2 - E_a^2)/m^2$, $\rho' = (m^2 - E_a^2 + q^2)/m^2$ and $p_0 = q_o = E_a$. The infrared divergences in $\Delta E_a^{\mathrm{ren(z)}}$ and $\Delta E_a^{\mathrm{ren(o)}}$ cancel in view of the Ward identity and the Dirac equation [12,13].

The expression for the many-potential term $\Delta E^{(\mathrm{m})}$ is both ultraviolet and infrared finite, but most difficult to evaluate numerically. It can be treated in the following way. The S-matrix element, corresponding to Figure 2m reads

$$\langle\Psi_a|S^{(4)}|\Psi_a\rangle = e^4 \int \overline{\Psi}_a(x_1)\gamma^{\mu_1} S^{(0)}(x_1x_2)\gamma^{\mu_2} eV_{\mu_2}(x_2)$$
$$\times S(x_2x_3)\gamma^{\mu_3} eV_{\mu_3}(x_3) S^{(0)}(x_3x_4)\gamma^{\mu_4}\Psi_a(x_4)$$
$$\times D_{\mu_1\mu_4}(x_1x_4) d^4x_1, ..., d^4x_4, \qquad (16)$$

where $V_\mu(x) = \delta_{\mu 4} V(\mathbf{x})$ is the nuclear potential, $S^{(0)}(x_1x_2)$ is the free electron propagator, $\mathcal{S}(x_2x_3)$ is the electron propagator in the external potential V_μ and $\mathcal{D}_{\mu_1\mu_4}(x_1x_4)$ is the photon propagator in an arbitrary gauge. The free photon propagator in the momentum space reads

$$\mathcal{D}_{\mu_1\mu_2}(k) = -\frac{1}{k^2}\left(g_{\mu_1\mu_2} - \frac{k_{\mu_1}k_{\mu_2}}{k^2}\right) - \frac{d_0}{k^2}\frac{k_{\mu_1}k_{\mu_2}}{k^2}. \qquad (17)$$

The most general expression for the many potential contribution to matrix element of the self-energy operator

appears as

$$\left\langle \Psi_a \left| \hat{\Sigma}^{\mathrm{ren(m)}} \right| \Psi_a \right\rangle = \left(\hat{\Sigma}^{\mathrm{ren(m)}}(E_a) \right)_{aa} = -\frac{\alpha}{\pi} \sum_m \int_0^\infty dw \mathcal{R}e \left\{ \sum_n \frac{1}{E_a - E_m - iw} \int \phi_m^+(-w, \mathbf{r}_1) \times \Psi_a(\mathbf{r}_2) \frac{1 - \boldsymbol{\alpha}_1 \boldsymbol{\alpha}_2}{r_{12}} e^{(-wr_{12})} \Psi_m(\mathbf{r}_1) \phi_a(w, \mathbf{r}_2) \, d^3 r_1 d^3 r_2 \right\}. \quad (18)$$

Here the summation over m is extended over the entire Dirac spectrum for the bound electron, $r_{12} = |\mathbf{r}_1 - \mathbf{r}_2|$ and $\boldsymbol{\alpha}_i$ are the Dirac matrices acting on the different wave functions. The function $\phi_m(\omega, \mathbf{r})$ is defined as:

$$\phi_m(\omega, \mathbf{r}) = \sum_\nu \frac{\left(\hat{V}\right)_{\nu m}}{E_m - E_\nu - i\omega} \Psi_\nu(\mathbf{r}), \quad (19)$$

where the sum over ν is the extended over the entire free Dirac spectrum, $\Psi_\nu(\mathbf{r})$ and E_ν denote the corresponding free eigenfunctions and eigenvalues of the Dirac equation.

Within the numerical B-spline approach [14] the electron propagator $S^{(0)}$ can be represented in the same way as the bound propagator, if one sets $Z = 0$. Equation (18) thus contains in total a triple summation over the Dirac spectrum. These summations can be performed numerically with modern computer facilities.

2.2 Vacuum-polarization correction

Apart from the one-loop electron self energy the another radiative correction the one-loop vacuum-polarization (VP) correction should be taken into account. After integrating over time and frequency variables in the S-matrix element corresponding to the VP correction (part (a) in Fig. 3) to the energy level $|a\rangle$ reads

$$\Delta E_a^{\mathrm{VP}} = \int \overline{\Psi}_a(\mathbf{r}_1) \gamma_0 V_{\mathrm{VP}}(\mathbf{r}_1) \Psi_a(\mathbf{r}_1) \, d^3 r_1, \quad (20)$$

where

$$V_{\mathrm{VP}}(\mathbf{r}_1) = e \int \frac{\rho_{\mathrm{VP}}(\mathbf{r}_2)}{|\mathbf{r}_1 - \mathbf{r}_2|} \, d^3 r_2 \quad (21)$$

is the vacuum-polarization potential generated by the induced vacuum-polarizations charge density

$$\rho_{\mathrm{VP}}(\mathbf{r}_2) = \frac{e}{2\pi} Tr \left(\int_{-\infty}^{\infty} \widehat{S}(\omega) \, \gamma_0 \, d\omega \right), \quad (22)$$

respectively. In equation (23) $\widehat{S}(\omega)$ is the temporal Fourier transform of the Green (resolvent) operator of the Dirac equation and the symbol Tr indicates the trace over the entire Dirac spectrum.

The first term of this expansion (Fig. 3b) vanishes in view of the the Furry theorem [15], according to which free electron loops with an odd number of vertices do not contribute. The divergency arrives in the second term of the expansion only (Fig. 3c), while the remainder term Figure 3d is finite.

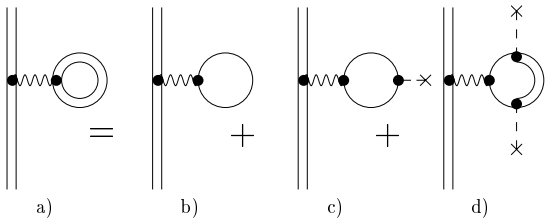

Fig. 3. The expansion of the VP graph in powers of the effective external potential V. Notations are the same as in Figure 2.

The contribution of the one-potential term can be represented in the form

$$\Delta E_a^{\mathrm{Ueh}} = \int d^3 r \, \overline{\Psi}_a(\mathbf{r}) \gamma_0 V_{\mathrm{Ueh}}(r) \Psi_a(\mathbf{r}) \, . \quad (23)$$

For a point nucleus the Uehling potential reads [16]

$$V_{\mathrm{Ueh}}(r) = \frac{2\alpha^2 Z}{3\pi r} \int_1^\infty e^{-2mr\chi} \left(1 + \frac{1}{\chi^2} \right) \frac{\sqrt{\chi^2 - 1}}{\chi^2} \, d\chi. \quad (24)$$

Here and below in equations (26, 27) the electron mass m is explicitly restored. For a point nucleus the asymptotic behavior of the Uehling potential is given by the expressions

$$V_{\mathrm{Ueh}}(r) = \frac{\alpha^2 Z}{r} \begin{cases} -\frac{1}{3\pi}[5/3 + 2C + 2\ln(mr)], & mr \ll 1 \\ \frac{1}{4\sqrt{\pi}} \frac{e^{-2mr}}{(mr)^{3/2}}, & mr \gg 1, \end{cases} \quad (25)$$

where C denotes Eulers' constant. Remembering that the Bohr radius in relativistic units is $r_0 = 1/m\alpha$, we see that at characteristic atomic distances in the neutral hydrogen atom ($Z = 1$) the deviation from the Coulomb potential is exponentially small, i.e. $V_{\mathrm{Ueh}}(r_0) \approx e^{-1/\alpha}$. However, this is not the case in hydrogenlike ions with large values of Z, where

$$V_{\mathrm{Ueh}}(r_0) \approx V_{\mathrm{Ueh}}(1/m\alpha Z) \approx e^{-1/\alpha Z}.$$

One can check that taking into account the Uehling term will be sufficient in the case of many-electron system. For extended nuclei the Uehling potential has to be replaced by the expression [17–19]:

$$V_{\mathrm{Ueh}}(\mathbf{r}) = -\frac{\alpha^2}{\pi} \int d^3 r' \rho(r') \int_1^\infty dt \sqrt{t^2 - 1} \times \left(\frac{2}{3t^2} + \frac{1}{3t^4} \right) \frac{e^{-2mt|\mathbf{r} - \mathbf{r}'|}}{|\mathbf{r} - \mathbf{r}'|}, \quad (26)$$

where $\rho(r')$ is the nuclear charge density.

For the latter we the Fermi distribution

$$\rho(r) = \frac{\rho_0}{1 + \exp\left[\frac{r - a_n}{c_n} \right]} \quad (27)$$

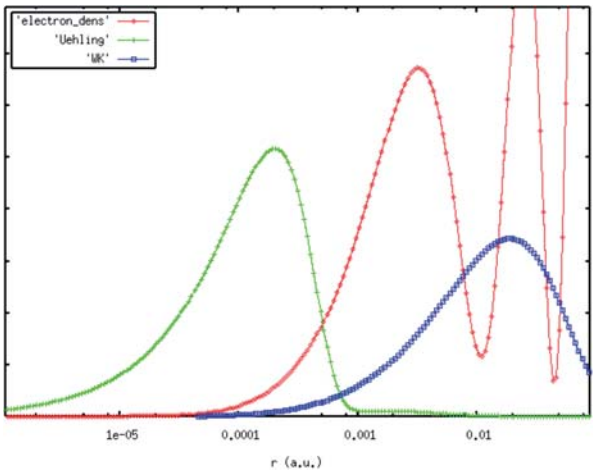

Fig. 4. (Color online) The graphs of the vacuum-polarization potentials corresponding to the Uehling and Wichmann-Kroll contributions are depicted together with the electron density for valence shell in Eka-Au. Compared with the Uehling term, the Wichmann-Kroll (WK) contribution is multiplied by a factor of 10^2.

is employed, where the parameters a_n and c_n are defined by the nuclear mass. ρ_0 can be computed via the expression

$$\rho_0 = \frac{3Z}{4c_n^3\mathcal{N}}. \tag{28}$$

The nuclear charge density $\rho(r)$ is defined by the normalization condition $\int d^3\mathbf{r}\rho(r) = Z$; the parameter $\mathcal{N}$ equals

$$\mathcal{N} = 1 + \pi^2\frac{a_n^2}{c_n^2} + 6\frac{a_n^3}{c_n^3}\sum_{k=1}^{\infty}\frac{(-1)^{n-1}}{k^3}e^{-ka_n/c_n}.$$

After the angular integration equation (27) takes the form [20]

$$V_{\rm Ueh}(\mathbf{r}) = -\frac{2\alpha^2}{3r}\int_0^\infty dx\; x\rho(x)\int_0^1 du\left(1-u^2\right)^{1/2} \times\left(1+\frac{u^2}{2}\right)\left(e^{-2|r-x|/(\alpha u)} - e^{-2(r+x)/(\alpha u)}\right) = S_{\rm Ueh}(r)/r. \tag{29}$$

The first evaluation of the remainder term to first all orders in αZ has been performed by Wichmann and Kroll [21]. For the purposes here it will sufficient to employ the next leading-order contribution to the Wichmann-Kroll potential $V_{\rm B}$ obtained by Blomqvist [22]

$$\Delta E_a^{\rm WKB} = \int d\mathbf{r}\,\Psi_a^+(\mathbf{r})V_B(r)\Psi_a(\mathbf{r}), \tag{30}$$

with the potential (which is depicted in Fig. 4 as well):

$$V_B(r) = \frac{\alpha(Z\alpha)^3}{\pi r}\int_0^\infty dt\, e^{-2tr}\frac{1}{t^4} \times\left\{-\frac{1}{12}\pi^2[t^2-1]^{1/2}\Theta(t-1) + \int_0^t dx\,[t^2-x^2]^{1/2}f(x)\right\}, \tag{31}$$

$$f(x) = -2x\psi(x^2) - x\ln(1-x^2) + \frac{1-x^2}{x^2} \times\ln\frac{1+x}{1-x}\ln(1-x^2) + \frac{1-x^2}{4x^2}\ln^2\frac{1+x}{1-x} + \frac{2-x^2}{x(1-x^2)}\ln(1-x^2) + \frac{3-2x^2}{1-x^2}\ln\frac{1+x}{1-x} - 3x, \quad x<1, \tag{32}$$

$$f(x) = x^{-2}\psi(x^{-2}) - \frac{3x^2+1}{2x}[\psi(x^{-1}) - \psi(-x^{-1})] -\frac{2x^2-1}{2x^2}\left[\ln^2(1-x^{-2}) + \ln^2\frac{x+1}{x-1}\right] -(2x-1)\ln(1-x^{-2})\ln\frac{x+1}{x-1} + \frac{3x^2+1}{4x}\ln^2\frac{x+1}{x-1} -2\ln x\ln(1-x^{-2}) - \frac{3x^2+1}{2x}\ln x\ln\frac{x+1}{x-1} + \left[5 - \frac{x(3x^2-2)}{x^2-1}\right]\ln(1-x^{-2}) + \left[\frac{3x^2+2}{x} - \frac{3x^2-2}{x^2-1}\right]\ln\frac{x+1}{x-1} + 3\ln x - 3, \quad x>1, \tag{33}$$

with the di-logarithmic function

$$\psi(x) = -\int_0^x dy\frac{\ln(1-y)}{y} = \sum_{n=1}^{\infty}\frac{x^n}{n^2}, \quad -1<x<1, \tag{34}$$

and $\Theta(x)$ as the usual step function. Although the Uehling term usually yields a fairly good approximation for the total VP on the level of 10%, nevertheless, accurate calculations for the valence electron levels in heavy elements should account for the higher-order Wichmann-Kroll term. In Figure 4 the dominant Uehling contribution and the higher-order Wichmann-Kroll contribution of the induced VP potential are displayed together with the radial density of the valence electrons in the Eka-Au atom.

3 QED effects within the frame of local potential and self-consistent approaches

In recent years relativistic atomic structure calculations for many-electron atoms have become increasingly more advanced. They comprise, for example, the Breit interactions and many multi-configuration methods. However, much less efforts have been made to take into account rigorously the QED effects to the energy of multi-electron levels or to account for the corresponding wave-function corrections. This may be due to the widespread opinion according to which the influences of QED corrections are negligible compared to relativistic and correlation effects. Although their evaluation is quite difficult to achieve one should consider this task, since they can indeed influence

Table 1. The binding energy for the valence electrons and corresponding QED corrections in superheavy atoms (in eV).

System	Eka-Au	Eka-Hg	Eka-Hg$^+$
$E_{7s}^{\rm DF}$	–11.4313	–12.2749	–21.2681
$E_{7s}^{\rm IP1}$	–10.6 [a]	–11.973 [b]	
$\Delta E_{7s}^{\rm SE,DF}$	8.87×10^{-2}	0.1024	0.1221
	8.66×10^{-2} [c]		
$\Delta E_{7s}^{\rm Ueh,DF}$	-3.24×10^{-2}	-3.81×10^{-2}	-4.29×10^{-2}
	-3.20×10^{-2} [c]		
$\Delta E_{7s}^{\rm Ueh,IP1}$	-3.14×10^{-2}	-3.51×10^{-2}	
$\Delta E_{7s}^{\rm Ueh,SCF.}$	-3.96×10^{-2}	-4.07×10^{-2}	-4.95×10^{-2}
$\Delta E_{7s}^{\rm WK,DF}$	1.66×10^{-4}	1.34×10^{-4}	9.23×10^{-5}
$\Delta E_{7s}^{\rm QED,DF}$	5.63×10^{-2}	6.43×10^{-2}	7.92×10^{-2}

[a] Reference [27], [b] reference [25], [c] reference [8].

chemical properties of superheavy atoms. The magnitude of QED corrections on valence-electron states could to be even larger as the uncertainties of the results obtained within different relativistic many-body approaches. This can be seen by performing calculations with and without implementation of QED radiative effects.

The remaining discrepancy between predictions for the valence-electron energy levels in Eka-Hg and according to the MPT [23] was of about -0.2 eV. This appears as the difference between a pure Dirac-Fock (DF) calculations for the level energy of $6d_{5/2}$ and $7s$ electrons, respectively. QED corrections may potentially help to improved the discrepancy. The sum of the SE and VP contributions raises the chemical activity. But the magnitude of this "asset" is of about 6×10^{-2} eV [8].

Reinvestigation of the absorption of Eka-Hg on a gold surface — without taking into account QED effects — predicted a chemical behavior between mercury (group 12 element) and a noble gas. See, for example, reference [24], which has been obtained within the framework of relativistic density-functional approach and later been confirmed by calculations presented in [25]. Inclusion of the total QED corrections could shift such prediction for chemical properties towards the behavior of a mercury homologue. The remaining energy difference between the level $6d_{5/2}$ and $7s$ obtained from RCC-SD calculations without QED amounts to 0.177 eV [26]. With QED corrections (see Tab. 1) this energy difference is of about 0.24 eV.

The first calculation of QED effects for a valence electron in Eka-Au has been presented in reference [8] within the effective local potential approach. Table 1 compiles the results of our present analysis. The first line of Table 1 presents our results for the Dirac Fock (DF) one-electron energies of the $7s$-states ($E_{7s}^{\rm DF}$). They are compared with the values of the corresponding first ionization potentials ($E_{7s}^{\rm IP1}$) obtained within the framework of multi-configuration methods. Compared with the more precise values $E_{7s}^{\rm IP1}$ the results obtained from DF calculations have an accuracy of about 7% for Eka–Au [27] and about 2% for Eka–Hg [25], respectively.

The next five lines of Table 1 display the major contributions of QED radiative corrections for the three systems under consideration. All values indicated with subscripts "DF" and "IP1" were calculated within the effective local-potential approach. As it was shown in reference [8] one has quite some freedom in formulating an effective local potential. In this work we employed the effective potential, which is obtained by inversion of the DF-equation (indicated in Appendix A). The parameter ε was chosen equal to the DF one-electron energy $E_{7s}^{\rm DF}$ when calculating the "DF" values and equal to the ionization potential $E_{7s}^{\rm IP1}$ in case of the "IP1" values.

The self-energy correction $\Delta E_{7s}^{\rm SE,DF}$ are presented in the 3rd line of the Table 1. In Uehling approximation the vacuum-polarization corrections $\Delta E_{7s}^{\rm Ueh,DF}$ and $\Delta E_{7s}^{\rm Ueh,IP1}$, obtained within the different approximations are shown in the 4th and 5th line, respectively. The Wichmann-Kroll (WK) corrections $\Delta E_{7s}^{\rm WK,DF}$ (Fig. 3d) given in the 7th line of Table 1 turn out to be rather small due to an additional factor of α^2. However, as a function of r the WK potential falls off of much slower (inverse power law) then Uehling term (exponential decrease), which is depicted in Figure 4. The total results for the one-loop QED corrections ($\Delta E_{7s}^{\rm QED,DF}$) are given in the last line of Table 1.

The 6th line in Table 1 presents the results of a self-consistent field (SCF) calculation including the leading Uehling correction (Fig. 3c) in the Dirac-Fock equations. The results for $\Delta E_{7s}^{\rm Ueh,SCF}$ should be compared with corresponding corrections $\Delta E_{7s}^{\rm Ueh,DF}$ to the DF energies (within the SCF approach we can use DF energies only). Implementation of the Uehling potential in the SCF procedure, respectively in the DF equation, yields significantly different results for the VP correction. The absolute value for the Uehling correction $\Delta E_{7s}^{\rm Ueh}$ increases by 22% for Eka-Au, 7% for Eka-Hg and 17% for Eka-Hg$^+$. A similar estimate for the SE correction is not so easy. The last line in Table 1 is the sum of the 3rd and 6th lines.

Note, that the Uehling potential can easily be implemented in post-DF methods, such as e.g. in the multi-configuration DF approach.

Based on the analysis presented in Table 1, we can conclude as follows: The one-loop QED corrections to the $7s$-state turn out to be considerably larger than the ones to the $6d$-state (see Ref. [28]). The result for the total QED corrections to the $7s$-state appear to be of the same order of magnitude as the differences between the energies between $7s-6d$ obtained from pure relativistic many-electron approaches [25] neglecting QED effects. This underlines the significance of QED-radiative effects on the energy of valance electrons in such superheavy systems. In particular, the QED effects for the valence electrons in Eka-Hg raise the chemical activity of this atom. The difference to more exact and complex evaluations of such effects is already near the inaccuracy of pure relativistic calculation without QED.

I.G. and I.T. are grateful to the Technical University of Dresden for hospitality during their visits in 2006. The authors acknowledge financial support from DFG.

Appendix A: Effective potentials for valence electrons

The effective local potential (V) can be expressed in terms of the radial wave function by inversion of the (radial) Dirac-Fock equations within the local-potential approximation. The Dirac equation with a local potential V reads

$$\left(-\frac{d}{dr}+\frac{\kappa}{r}\right)F(r)+V(r)G(r)=\varepsilon G(r)$$
$$\left(\frac{d}{dr}+\frac{\kappa}{r}\right)G(r)+[V(r)-2m]F(r)=\varepsilon F(r), \quad (35)$$

where G and F are the large and small components of the wave function, respectively, κ is the relativistic quantum number and $\varepsilon = E_{n\kappa} - m$. These equations allow for the derivation of an approximate effective potential via inversion of the first equation for the the large component employing Dirac-Fock wave functions ($G^{\rm DF}, F^{\rm DF}$)

$$V(r)=\frac{\left(\frac{d}{dr}-\frac{\kappa}{r}\right)F^{\rm DF}(r)+\varepsilon G^{\rm DF}(r)}{G^{\rm DF}(r)}. \quad (36)$$

We should mention that the potential used in the calculations has been smoothed in the vicinity of the nodes of the wave function $G^{\rm DF}$. In the present calculations of the QED corrections the corresponding potential for the $7s$-state has been used.

References

1. R. Eichler et al., Nature **407**, 63 (2000)
2. Ch.E. Düllmann et al., Nature **418**, 859 (2002); V. Pershina, T. Bastug, B. Fricke, S. Vagra, J. Chem. Phys. **115**, 792 (2001)
3. S. Hoffman et al., Eur. Phys. J. A **14**, 147 (2002)
4. Yu.Ts. Oganessian et al., Phys. Rev. C **62**, 041604 (2000)
5. A.B. Yakushev, Nucl. Phys. A **734**, 204 (2004)
6. P. Roy Chowdhury, C. Samanta, D.N. Basu, Phys. Rev. C **73**, 014612 (2006)
7. T.C. Tucker, L.D. Roberts, C.W. Nestor Jr, T.A. Carlson, F.B. Malik, Phys. Rev. **174**, 118 (1968)
8. L. Labzowsky, I. Goidenko, M. Tokman, P. Pyykkö, Phys. Rev. A **59**, 2707 (1999)
9. S. Fritzsche, Eur. Phys. J. D **33**, 15 (2005)
10. G.E. Brown, H.S. Langer, G.W. Schäfer, Proc. Roy. Soc. A **251**, 92 (1959); G.E. Brown, D.F. Mayers, Proc. Roy. Soc. A **251**, 105 (1959)
11. N.N. Bogoljubov, D.V. Shirkov, *Introduction to the Theory of the Quantized Fields* (New York, Wiley, 1959)
12. H.J. Snyderman, Ann. Phys. NY **211**, 43 (1991)
13. L.N. Labzowsky, Zh. Eksp. Teor. Fiz **59**, 167 (1970) [Engl. Transl.: Sov. Phys. JETP **32**, 1171 (1970)]
14. W.R. Johnson, S.A. Blundell, J. Sapirstein, Phys. Rev. A **37**, 307 (1988)
15. W.H. Furry, Phys. Rev. **51**, 125 (1937)
16. E.A. Uehling, Phys. Rev. **48**, 55 (1935)
17. S. Klarsfeld, Phys. Lett. B **66**, 86 (1977)
18. S.A. Blundell, Phys. Rev. A **46**, 3762 (1992)
19. H. Persson, I. Lindgren, S. Salomonson, P. Sunnergren, Phys. Rev. A **48**, 2772 (1993)
20. L.W. Fullton, G.A. Rinker Jr, Phys. Rev. A **13**, 1283 (1976); K.H. Huang, Phys. Rev. A **14**, 1311 (1976)
21. E. Wichmann, N.M. Kroll, Phys. Rev. **101**, 843 (1956)
22. J. Blomqvist, Nucl. Phys. B **48**, 95 (1972)
23. K. Pitzer, J. Chem. Phys. **63**, 1033 (1975)
24. V. Pershina, T. Bastug, C. Sarpe-Tudoran, J. Anton, B. Fricke, Nucl. Phys. A **734**, 200 (2004)
25. N.S. Mosyagin, T.A. Isaev, A.V. Titov, J. Chem. Phys. **124**, 224302 (2006)
26. N.S. Mosyagin, A.N. Petrov, A.V. Titov, I.I. Tupitsyn, in: *Progress in Theoretical Chemistry and Physics*, Part II (Springer, Berlin, 2006), Vol. 15, pp. 229–252; see also: `arXiv.org/physics/0505207` (2005)
27. E. Eliav, U. Kaldor, P. Schwerdtfeger, B.A. Hess, Ya. Ishikawa, Phys. Rev. Lett. **73**, 3203 (1994)
28. J. Sapierstein, K.T. Cheng, Phys. Rev. A **73**, 012503 (2005)